

To appear in *Molecular Physics*  
Vol. 00, No. 00, Month 200x, 1–26

## RESEARCH ARTICLE

### *Ab initio* potential energy surface for the nitrogen molecule pair and thermophysical properties of nitrogen gas

Robert Hellmann\*

Institut für Chemie, Universität Rostock, D-18059 Rostock, Germany

(Received 00 Month 200x; final version received 00 Month 200x)

A four-dimensional potential energy hypersurface (PES) for the interaction of two rigid nitrogen molecules was determined from high-level quantum-chemical *ab initio* computations. A total of 408 points for 26 distinct angular configurations were calculated utilizing the counterpoise-corrected supermolecular approach at the CCSD(T) level of theory and basis sets up to aug-cc-pV5Z supplemented with bond functions. The calculated interaction energies were extrapolated to the complete basis set limit and complemented by corrections for core-core and core-valence correlations, relativistic effects and higher coupled-cluster levels up to CCSDT(Q). An analytical site-site potential function with five sites per nitrogen molecule was fitted to the interaction energies. The PES was validated by computing second and third pressure virial coefficients as well as shear viscosity and thermal conductivity in the dilute-gas limit. An improved PES was obtained by scaling the CCSDT(Q) corrections for all 408 points by a constant factor, leading to quantitative agreement with the most accurate experimental values of the second virial coefficient over a wide temperature range. The comparison with the best experimental data for shear viscosity shows that the values computed with the improved PES are too low by about 0.3% between 300 and 700 K. For thermal conductivity large systematic deviations are found above 500 K between the calculated values and most of the experimental data.

**Keywords:** nitrogen pair potential; *ab initio* calculations; kinetic theory; virial coefficients; transport properties

This is an Accepted Manuscript of an article published by Taylor & Francis in *Molecular Physics* on 28/09/2012, available online: <http://www.tandfonline.com/10.1080/00268976.2012.726379>.

#### 1. Introduction

The calculation of thermophysical properties of fluids requires precise knowledge of the intermolecular potentials between individual molecules. Especially pair po-

---

\*Email: robert.hellmann@uni-rostock.de

tentials can be predicted with high accuracy for substances composed of atoms [1–6] or small molecules, such as methane [7], water [8] or hydrogen sulfide [9] using quantum-chemical *ab initio* methods. For low-density gases the thermophysical properties are governed solely by binary interactions, so that once the pair potentials are available, it is straightforward to calculate the second pressure virial coefficient using statistical thermodynamics or the transport properties in the limit of zero density utilizing the kinetic theory of gases [10].

At higher densities many-body effects have a strong influence on macroscopic properties. One way to account for this is the implicit inclusion of many-body effects into the pair potentials. These so-called effective pair potentials are typically adjusted to structural information of the molecules and accurate experimental data for bulk properties. In molecular simulations the most commonly used effective pair potential models for molecular nitrogen are site-site potentials with Lennard-Jones sites on the atoms and with a point-quadrupole at the centre of mass [11], or, alternatively, with partial charges on the atoms and at the centre of mass to represent the quadrupole moment [12]. Since effective pair potentials do not represent the underlying physics of the interactions correctly, their predictive capability is limited. The other possibility of accounting for nonadditive contributions is to combine pure pair potentials with explicit nonadditive three-body potentials, which can also be determined with quantum-chemical *ab initio* methods, see, for example, [13, 14].

*Ab initio* nonadditive three-body potentials for molecular nitrogen have not yet become available. However, several pair potentials based on quantum-chemical *ab initio* calculations have been developed since the 1980s.

One of the first was developed by Böhm and Ahlrichs [15]. They calculated 46 points on the intermolecular potential energy hypersurface (PES) using the supermolecular approach at the CPF level [16] with a [6s4p2d] basis set. A site-site potential function with three sites per molecule and five adjustable parameters was fitted to the computed interaction energies. An improved version of the potential was obtained by readjusting the dispersion contribution of the potential function to experimental values for the second virial coefficient. Both versions of the potential were used for molecular dynamics simulations of liquid nitrogen.

Van der Avoird *et al.* [17] used Hartree–Fock (HF) wave functions of nitrogen monomers, obtained with the [6s4p2d] basis set already employed by Böhm and Ahlrichs, to compute the first-order electrostatic and exchange interaction energies for 225 points. Utilizing *ab initio* dispersion coefficients [18], a spherical harmonics expansion of the  $N_2$ – $N_2$  intermolecular PES was constructed. Two scaling parameters were introduced to adjust the potential function to experimental data for the second virial coefficient. The potential was used for the calculation of several solid state properties. Later, Cappelletti *et al.* [19] further improved the potential function by readjusting five of its parameters in a multi-property fit to experimen-

tal data for the second virial coefficient, scattering cross sections and zero-density transport properties.

Amovilli and McWeeny [20] utilized a matrix partitioning approach to obtain  $N_2$ - $N_2$  interaction energies for six angular configurations from HF and TDHF (time-dependent Hartree-Fock) wave functions of the nitrogen monomers. They used a site-site potential function with nine sites per molecule to express the PES analytically. Scaling of the dispersion contribution by a factor of 1.2 was necessary to achieve reasonable agreement with experimental second virial coefficient values.

Stallcop and Partridge [21] applied the highly accurate coupled-cluster method with single, double and noniterative triple excitations (CCSD(T) [22]) and a [6s5p4d] basis set to compute a large number of points on the PES. They fitted an analytical function based on spherical harmonics expansions to the interaction energies and used experimental data for the second virial coefficient to adjust several parameters of the potential function.

Leonhard and Deiters [23] performed CCSD(T) calculations with the aug-cc-pVDZ and aug-cc-pVTZ basis sets [24, 25] for 126 points. They extrapolated the resulting interaction energies to the complete basis set (CBS) limit and fitted a site-site potential function with five sites per molecule to the CBS energies. Two scaling parameters were introduced to adjust the potential function to experimental values for the second virial coefficient. The potential was applied in Monte Carlo simulations of vapor-liquid equilibria. In these simulations different approximate nonadditive three-body potentials were tested. Surprisingly, the best agreement with experimental data was achieved when only the pair potential was used. The authors suspected that this might be due to a fortuitous cancellation of errors.

Karimi-Jafari *et al.* [26] calculated  $N_2$ - $N_2$  interaction energies for a large number of points at the MP2 level of theory with basis sets up to cc-pVQZ and extrapolated them to the CBS limit. An analytical potential function based on spherical harmonics expansions was fitted to the interaction energies, but not validated against thermophysical properties.

Gomez *et al.* [27] applied symmetry-adapted perturbation theory (SAPT) and a [5s3p2d1f] basis set to calculate a large number of points on the PES. A spherical harmonics expansion was fitted to the interaction energies and used to calculate second virial coefficients as well as integral scattering cross sections. Although the computed values for the second virial coefficient turned out to be too negative compared with experimental data, no adjustments to the potential function were performed.

Strąk and Krukowski [28] computed 315 points at the CCSD(T) level of theory with the aug-cc-pVQZ basis set. However, they did not correct the calculated interaction energies for the basis set superposition error (BSSE). The PES was expressed analytically by a spherical harmonics expansion and used for molecular dynamics

simulations of nitrogen under very high pressures.

The new *ab initio* pair potential presented in this paper is based on supermolecular CCSD(T) calculations for more than 400 points. Basis sets up to quintuple-zeta quality with bond functions were applied and the resulting interaction energies extrapolated to the CBS limit. In addition, corrections for core-core and core-valence correlations, relativistic effects and higher coupled-cluster levels up to CCSDT(Q) [29] were determined. A five-centre site-site potential function with isotropic site-site interactions was fitted to the calculated interaction energies. Both the site-site interaction parameters and the positions of the sites were fully optimized. We chose the site-site potential model because of its simplicity, which makes it easy to use when calculating macroscopic properties by means of molecular simulations.

The PES was validated by computing several thermophysical properties of nitrogen gas. The second and third pressure virial coefficients were calculated classically with the full first-order quantum corrections. A small adjustment of the pair potential to the most accurate experimental data for the second virial coefficient was performed. Nonadditive three-body contributions to the third virial coefficient were taken into account by an Axilrod–Teller–Muto potential with two sites per molecule and by the leading nonadditive induction contribution. The viscosity and the thermal conductivity in the dilute-gas limit were computed using the kinetic theory of gases for linear molecules [10, 30] and the classical trajectory approach.

In Section 2, the *ab initio* computations for the nitrogen molecule pair as well as the analytical functions for the pair potential and the nonadditive three-body potential are described. In Section 3, the methodology for the calculation of the second and third pressure virial coefficients is discussed, and the computed values are compared with the most accurate experimental data. The calculations for viscosity and thermal conductivity in the dilute-gas limit are summarized in Section 4. The results are again compared with experimental data.

## 2. Intermolecular potential

### 2.1. *Ab initio* calculations

The intermolecular potential  $V_{12}$  between two nitrogen molecules is a six-dimensional PES if both intermolecular and intramolecular degrees of freedom are considered. The dimensionality is reduced to four if the  $N_2$  molecules are approximated as rigid rotors. Past experience with different small molecules shows that a highly accurate intermolecular PES can be constructed if the zero-point vibrationally averaged geometry is used for the rigid monomers, see, for example, [7–9, 31]. We determined the zero-point vibrationally averaged bond length of  $N_2$  as follows. First, a geometry optimization was performed at the all-electron CCSD(T) level with the cc-pwCVQZ basis set [32], resulting in an equilibrium bond length of

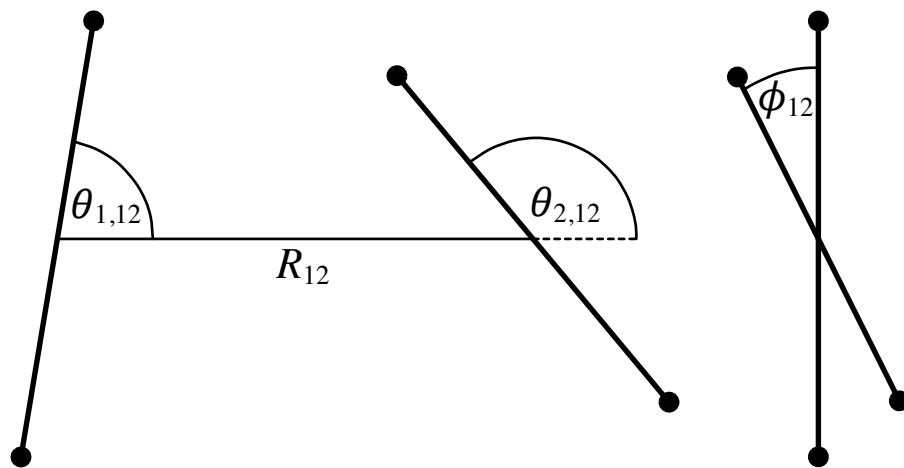


Figure 1. Internal coordinates of the nitrogen molecule pair.

1.0979 Å. Then a cubic force field calculation at the same level of theory was performed, yielding a vibrationally averaged bond-length of 1.1016 Å. The difference between these two values was then added to the experimental value of 1.0977 Å for the equilibrium bond length [33]. The resulting value of 1.1014 Å for the zero-point vibrationally averaged bond length was utilized for all further calculations. In the cubic force field calculation the difference between the equilibrium quadrupole moment and the vibrationally averaged quadrupole moment was also determined, as it was needed for the construction of the analytical pair potential function (see Section 2.2).

Each configuration of two rigid N<sub>2</sub> molecules can be conveniently expressed by the four variables  $R_{12}$ ,  $\theta_{1,12}$ ,  $\theta_{2,12}$  and  $\phi_{12}$  (illustrated in Figure 1), where  $R_{12}$  is the distance between the centres of mass of molecules 1 and 2,  $\theta_{1,12}$  and  $\theta_{2,12}$  are the angles between the  $R_{12}$  axis and the bond axes of molecules 1 and 2, respectively, and  $\phi_{12}$  is the dihedral angle. The angles can be restricted to  $0^\circ \leq \theta_{2,12} \leq \theta_{1,12} \leq 90^\circ$  and  $0^\circ \leq \phi_{12} \leq 180^\circ$  due to symmetry. Altogether 26 distinct angular configurations were considered. The first 14 angular configurations resulted from varying all three angles in steps of  $45^\circ$ , starting with  $0^\circ$ . The remaining 12 angular configurations were obtained by varying all three angles in steps of  $45^\circ$ , starting with  $22.5^\circ$ . Sixteen centre-of-mass separations between 2.25 Å and 8.0 Å were considered, leading to a total of 416 ( $26 \times 16$ ) configurations. Eight configurations, where two atoms from different molecules were too close to each other, had to be discarded.

For all configurations the interaction energies  $V_{12}(R_{12}, \theta_{1,12}, \theta_{2,12}, \phi_{12})$  were calculated using the supermolecular approach including the full counterpoise correction [34] at the frozen-core CCSD(T) level with the aug-cc-pVXZ basis sets [24, 25] for  $X = 4$  and  $X = 5$ . Both basis sets were augmented by a small  $3s3p2d1f$  set of bond functions located midway along the  $R_{12}$  axis. The exponents of the bond functions are 0.1, 0.3 and 0.9 for both  $s$  and  $p$ , 0.25 and 0.75 for  $d$  and 0.45 for  $f$ . The correla-

tion parts of the interaction energies,  $V_{12}^{\text{CCSD(T) corr}}$ , computed with these two basis sets, were extrapolated to the CBS limit with the two-point extrapolation scheme proposed by Halkier *et al.* [35],

$$V_{12}^{\text{CCSD(T) corr}}(X) = V_{12,\text{CBS}}^{\text{CCSD(T) corr}} + \alpha X^{-3}. \quad (1)$$

The HF interaction energies were not extrapolated because the differences between the results for the two basis sets are already very small. Therefore, the HF interaction energies from the aug-cc-pV5Z calculations were used to approximate the CBS limit.

Corrections for core-core and core-valence correlations, relativistic effects and higher coupled-cluster levels up to CCSDT(Q) were computed for all configurations and added to the non-relativistic frozen-core CCSD(T) interaction energies in the CBS limit:

$$V_{12} = V_{12,\text{CBS}}^{\text{CCSD(T)}} + \Delta V_{12}^{\text{core}} + \Delta V_{12}^{\text{rel}} + \Delta V_{12}^{\text{CCSDT(Q)}}. \quad (2)$$

The corrections for core-core and core-valence correlations,  $\Delta V_{12}^{\text{core}}$ , were determined at the CCSD(T) level with the aug-cc-pwCVTZ basis set [32] by calculating the differences between the interaction energies obtained with all electrons correlated and the interaction energies obtained within the frozen-core approximation. The relative contributions of  $\Delta V_{12}^{\text{core}}$  to the well depths of the 26 angular configurations are in most cases within  $\pm 0.5\%$ . The corrections for relativistic effects,  $\Delta V_{12}^{\text{rel}}$ , were computed utilizing second-order direct perturbation theory (DPT2) [36, 37] at the frozen-core CCSD(T) level with the aug-cc-pwCVTZ basis set. They are similar in magnitude to the corrections for core-core and core-valence correlations. The corrections for higher coupled-cluster levels up to CCSDT(Q),  $\Delta V_{12}^{\text{CCSDT(Q)}}$ , were obtained by calculating the differences between the frozen-core CCSDT(Q) and CCSD(T) interaction energies applying the aug-cc-pVDZ basis set. Unfortunately, we could not use a larger basis set due to the enormous computational costs of the CCSDT(Q) method. The relative contributions of  $\Delta V_{12}^{\text{CCSDT(Q)}}$  to the well depths of the 26 angular configurations vary between +1.1% and +3.2%. If the computationally less demanding CCSDT method is used instead of the CCSDT(Q) method, the relative contributions are of similar magnitude but with opposite sign.

The results of the *ab initio* calculations for the 408 configurations of two nitrogen molecules can be found in the supplementary material. The CFOUR program [38] was employed for all CCSD(T) calculations. The CCSDT(Q) calculations were carried out using the general coupled-cluster code MRCC of Kállay [39].

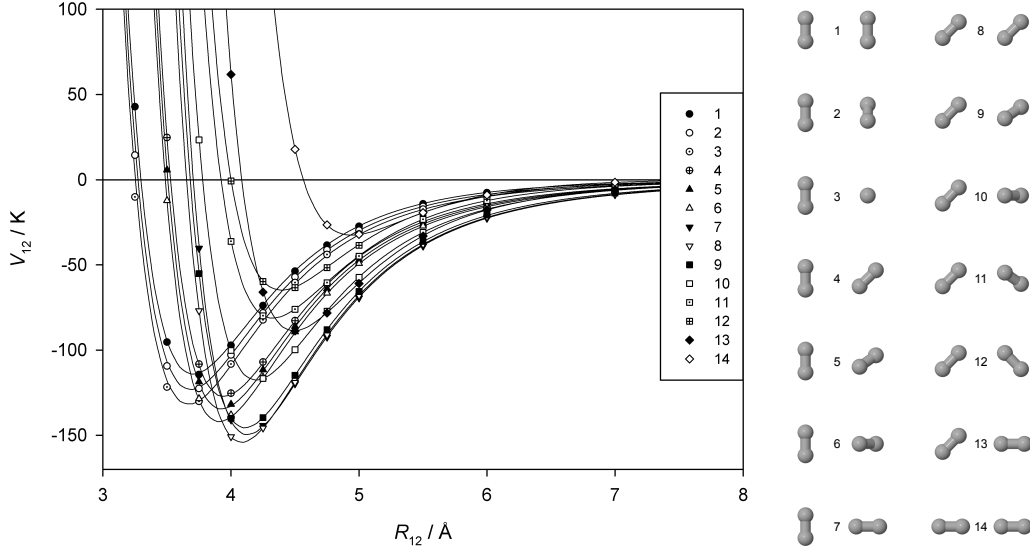


Figure 2.  $N_2$ - $N_2$  pair potential as a function of the distance  $R_{12}$  for the first 14 of the 26 considered angular configurations. The *ab initio* calculated values (with  $\Delta V_{12}^{CCSDT(Q)}$  scaled by 0.5, see text) are represented by symbols and the fitted analytical potential function  $V_{12}^B$  by solid lines.

## 2.2. Analytical pair potential function

A site-site potential function with five sites per molecule was fitted to the computed interaction energies. This corresponds to three different types of sites and six different types of site-site combinations. The functional form used for each site-site interaction is

$$V_{12,ij}(R_{12,ij}) = A_{ij} \exp(-\alpha_{ij} R_{12,ij}) - f_6(b_{ij}, R_{12,ij}) \frac{C_{6ij}}{R_{12,ij}^6} + \frac{q_{1,i} q_{2,j}}{R_{12,ij}}, \quad (3)$$

where  $R_{12,ij}$  is the distance between site  $i$  in molecule 1 and site  $j$  in molecule 2. The damping function  $f_6$  is given by [40]

$$f_6(b, R) = 1 - \exp(-bR) \sum_{k=0}^6 \frac{(bR)^k}{k!}. \quad (4)$$

The total interaction potential is the sum over all 25 site-site interactions,

$$V_{12}(R_{12}, \theta_{1,12}, \theta_{2,12}, \phi_{12}) = \sum_{i=1}^5 \sum_{j=1}^5 V_{12,ij} [R_{12,ij}(R_{12}, \theta_{1,12}, \theta_{2,12}, \phi_{12})]. \quad (5)$$

The parameters  $A$ ,  $\alpha$ ,  $b$  and  $C_6$  for the six different site-site combinations as well as the site charges  $q$  and the positions of the sites were fully optimized in a non-linear least-squares fit to the 408 *ab initio* interaction energies. Even though the chosen functional form does not account for higher-order dispersion coefficients like  $C_8$ , it is still flexible enough to fit the *ab initio* interaction energies very accurately. Three

constraints were imposed: (i) the total charge of the monomers had to be zero; (ii) the isotropic average of the  $C_6$  dispersion coefficient,  $C_{6\text{iso}} = \sum_{i=1}^5 \sum_{j=1}^5 C_{6ij}$ , had to be equal to the accurate value of 73.39 a.u. [41] from dipole oscillator strength distributions (DOSDs); (iii) the quadrupole moment of the monomers had to be equal to the zero-point vibrationally averaged value of  $-1.1202$  a.u. We obtained this value by adding the difference between the equilibrium quadrupole moment and the vibrationally averaged quadrupole moment (see Section 2.1) to the highly accurate *ab initio* value of  $-1.1273$  a.u. [42] for the equilibrium quadrupole moment.

The potential function thus obtained is denoted by  $V_{12}^A$ . Using the most accurate experimental data for the second virial coefficient as guidance (see Section 3.3), an improved potential function,  $V_{12}^B$ , resulted after scaling  $\Delta V_{12}^{\text{CCSDT(Q)}}$  by a factor of 0.5 for all 408 interaction energies used for the fit. This should be a reasonable procedure in view of the questionable accuracy of  $\Delta V_{12}^{\text{CCSDT(Q)}}$  (see Section 2.1). Figure 2 illustrates the distance dependence of the *ab initio* calculated values (with  $\Delta V_{12}^{\text{CCSDT(Q)}}$  scaled by 0.5) and of the fitted analytical potential function  $V_{12}^B$  for the first 14 of the 26 considered angular configurations. The interaction energies are given in Kelvin, i.e., they have been divided by Boltzmann’s constant  $k_B$ . The parameters for both potential functions as well as the interaction energies calculated with these functions for all 408 investigated configurations are given in the supplementary material.

The equilibrium geometries for  $V_{12}^A$  and  $V_{12}^B$  are  $R_{12} = 3.9938 \text{ \AA}$ ,  $\theta_{1,12} = \theta_{2,12} = 50.08^\circ$ ,  $\phi_{12} = 0^\circ$  with  $D_e = 158.54 \text{ K}$  and  $R_{12} = 3.9954 \text{ \AA}$ ,  $\theta_{1,12} = \theta_{2,12} = 50.13^\circ$ ,  $\phi_{12} = 0^\circ$  with  $D_e = 157.14 \text{ K}$ , respectively. This is in good agreement with the results of Cappelletti *et al.* [19] ( $R_{12} = 4.0 \text{ \AA}$ ,  $\theta_{1,12} = 49^\circ$ ,  $\theta_{2,12} = 50^\circ$ ,  $\phi_{12} = 0^\circ$ ,  $D_e = 150 \text{ K}$ ) and Karimi-Jafari *et al.* [26] ( $R_{12} = 4.1 \text{ \AA}$ ,  $\theta_{1,12} = \theta_{2,12} = 50^\circ$ ,  $\phi_{12} = 0^\circ$ ,  $D_e = 154.0 \text{ K}$ ). The *ab initio* potential of Karimi-Jafari *et al.* seems to benefit from a fortuitous cancellation of errors, since neither the MP2 method nor the cc-pVXZ basis sets (which do not have diffuse functions) are well suited to accurately determine the interaction energies between two nitrogen molecules. Interestingly, the two recent *ab initio* potentials of Gomez *et al.* [27] and of Strąk and Krukowski [28] differ significantly from  $V_{12}^A$  and  $V_{12}^B$ . The SAPT potential of Gomez *et al.* exhibits a slightly different equilibrium structure with a much stronger binding energy ( $R_{12} = 4.05 \text{ \AA}$ ,  $\theta_{1,12} = \theta_{2,12} = 45^\circ$ ,  $\phi_{12} = 0^\circ$ ,  $D_e = 171.7 \text{ K}$ ). This is due to the limitations of the second-order SAPT method, which is inferior to the CCSD(T) method. The potential of Strąk and Krukowski predicts the global minimum for  $R_{12} = 3.49 \text{ \AA}$ ,  $\theta_{1,12} = \theta_{2,12} = \phi_{12} = 90^\circ$  with  $D_e = 196.0 \text{ K}$ . This severe overestimation of the binding energy, despite the use of the CCSD(T) method and the relatively large aug-cc-pVQZ basis set, is due to the fact that Strąk and Krukowski did not apply the counterpoise correction [34] to avoid the basis set superposition error (BSSE). Therefore, we believe that  $V_{12}^B$  is the most accurate

representation of the  $N_2$ - $N_2$  interaction potential to date.

### 2.3. Nonadditive three-body potential

The total interaction potential between three molecules,  $V_{123}$ , can be written as the sum of the three pair interactions and a nonadditive three-body potential,  $\Delta V_{123}$ ,

$$V_{123} = V_{12} + V_{13} + V_{23} + \Delta V_{123}. \quad (6)$$

In the present work  $\Delta V_{123}$  is needed for the accurate determination of the third pressure virial coefficient (see Section 3). Since an *ab initio* nonadditive three-body potential for nitrogen is not yet available, we constructed an approximate three-body potential, taking into account contributions for nonadditive dispersion and nonadditive induction interactions:

$$\Delta V_{123} = \Delta V_{123}^{\text{disp}} + \Delta V_{123}^{\text{ind}}. \quad (7)$$

The nonadditive dispersion contribution,  $\Delta V_{123}^{\text{disp}}$ , is approximated by a sum of Axilrod–Teller–Muto interactions [43, 44] between triplets of nitrogen atoms, each of which is in a different molecule. The atoms in each molecule are referred to as sites 6 and 7. Hence

$$\Delta V_{123}^{\text{disp}} = \frac{C_{9\text{iso}}}{8} \sum_{i=6}^7 \sum_{j=6}^7 \sum_{k=6}^7 \frac{1 + 3 \cos \theta_{1,i} \cos \theta_{2,j} \cos \theta_{3,k}}{R_{12,ij}^3 R_{13,ik}^3 R_{23,jk}^3}, \quad (8)$$

where  $\theta_{1,i}$ ,  $\theta_{2,j}$  and  $\theta_{3,k}$  are the interior angles of the triangle formed by the sites, and  $C_{9\text{iso}} = 619.93$  a.u. [45] is the isotropic average of the triple-dipole dispersion coefficient of  $N_2$ .

The nonadditive induction potential,  $\Delta V_{123}^{\text{ind}}$ , can be written as

$$\Delta V_{123}^{\text{ind}} = \Delta V_{1,23}^{\text{ind}} + \Delta V_{2,13}^{\text{ind}} + \Delta V_{3,12}^{\text{ind}}, \quad (9)$$

with

$$\begin{aligned} \Delta V_{1,23}^{\text{ind}} &= -\frac{\alpha_{\text{iso}}}{2} \sum_{i=6}^7 \left[ \left( \sum_{j=1}^5 \mathbf{E}_{1,i;2,j} \right) \cdot \left( \sum_{k=1}^5 \mathbf{E}_{1,i;3,k} \right) \right] \\ &= -\frac{\alpha_{\text{iso}}}{2} \sum_{i=6}^7 \left[ \left( \sum_{j=1}^5 q_{2,j} \frac{\mathbf{R}_{12,ij}}{R_{12,ij}^3} \right) \cdot \left( \sum_{k=1}^5 q_{3,k} \frac{\mathbf{R}_{13,ik}}{R_{13,ik}^3} \right) \right] \end{aligned} \quad (10)$$

and analogous expressions for  $\Delta V_{2,13}^{\text{ind}}$  and  $\Delta V_{3,12}^{\text{ind}}$ . Here,  $\Delta V_{1,23}^{\text{ind}}$  is the contribution due to dipole moments on the polarizable sites 6 and 7 (assumed to have isotropic

dipole polarizabilities) of molecule 1 induced by the partial charges of molecules 2 and 3;  $\alpha_{\text{iso}} = 11.74$  a.u. [41] is the isotropic dipole polarizability of  $\text{N}_2$ ;  $\mathbf{E}_{1,i;2,j}$  is the electric field at site  $i$  in molecule 1 generated by the partial charge  $q_{2,j}$  of site  $j$  in molecule 2.

### 3. Second and third pressure virial coefficients

#### 3.1. Theory

The second pressure virial coefficient of a classical gas as a function of temperature is given by

$$B_2^{\text{cl}}(T) = -\frac{1}{2V} \int \cdots \int \langle f_{12} \rangle d\mathbf{R}_1 d\mathbf{R}_2, \quad (11)$$

where  $V$  is the volume,  $f_{12} = \exp(-V_{12}/k_{\text{B}}T) - 1$  is the two-particle Mayer function, and the angle brackets denote an average over all angular configurations of the molecules. If the potential is assumed to be pairwise additive ( $\Delta V_{123} = 0$ ), the classical third pressure virial coefficient can be written as

$$B_{3,\text{add}}^{\text{cl}}(T) = -\frac{1}{3V} \int \cdots \int \langle f_{12} f_{13} f_{23} \rangle d\mathbf{R}_1 d\mathbf{R}_2 d\mathbf{R}_3. \quad (12)$$

If nonadditive contributions are included, we obtain

$$B_{3,\text{nadd}}^{\text{cl}}(T) = -\frac{1}{3V} \int \cdots \int \langle f_{123} - f_{12} - f_{13} - f_{23} - f_{12}f_{13} - f_{12}f_{23} - f_{13}f_{23} \rangle \\ \times d\mathbf{R}_1 d\mathbf{R}_2 d\mathbf{R}_3, \quad (13)$$

where  $f_{123} = \exp(-V_{123}/k_{\text{B}}T) - 1$  is the three-particle Mayer function, see also [46, 47].

At low temperatures the assumption of classical molecules is no longer valid. However, if the system under study is not too far from classical conditions, quantum effects may be treated as quantum corrections to the classical value of any thermodynamic property. The first-order quantum correction to  $B_2^{\text{cl}}$  for rigid molecules is available [48, 49]. However, to the best of our knowledge, the first-order quantum correction to  $B_3^{\text{cl}}$  was derived for monatomic gases only [46].

We derived an expression for the first-order quantum correction to  $B_{3,\text{add}}^{\text{cl}}$  for linear molecules, starting from the configuration integral with first-order translational and rotational quantum corrections for  $N$  linear molecules,

$$Z_N = \int \cdots \int \left\langle \exp\left(-\frac{V_N}{k_{\text{B}}T}\right) - q_N \right\rangle d\mathbf{R}_1 \cdots d\mathbf{R}_N \quad (14)$$

with  $q_N = q_N^{\text{tr}} + q_N^{\text{rot}}$ , where

$$q_N^{\text{tr}} = \frac{\hbar^2}{12(k_{\text{B}}T)^2} \exp\left(-\frac{V_N}{k_{\text{B}}T}\right) \sum_{i=1}^N \frac{1}{m_i} \left( \nabla_{\text{tr},i}^2 V_N - \frac{1}{2k_{\text{B}}T} (\nabla_{\text{tr},i} V_N)^2 \right) \quad (15)$$

and

$$q_N^{\text{rot}} = \frac{\hbar^2}{12(k_{\text{B}}T)^2} \exp\left(-\frac{V_N}{k_{\text{B}}T}\right) \sum_{i=1}^N \frac{1}{I_i} \left( \nabla_{\text{rot},i}^2 V_N - \frac{1}{2k_{\text{B}}T} (\nabla_{\text{rot},i} V_N)^2 \right), \quad (16)$$

see, for example, [50]. Here,  $\hbar$  is Planck's constant divided by  $2\pi$ ;  $m_i$  and  $I_i$  are the mass and moment of inertia, respectively, of molecule  $i$ . To simplify Equation (15) we use Cartesian coordinates and assume that the potential is pairwise additive. Upon integration by parts we obtain

$$\int_{-\infty}^{\infty} \exp\left(-\frac{V_N}{k_{\text{B}}T}\right) \frac{\partial^2 V_N}{\partial x_i^2} dx_i = \frac{1}{k_{\text{B}}T} \int_{-\infty}^{\infty} \exp\left(-\frac{V_N}{k_{\text{B}}T}\right) \left( \frac{\partial V_N}{\partial x_i} \right)^2 dx_i \quad (17)$$

and similar relations with  $y_i$  and  $z_i$ , which we utilize to redefine  $q_N^{\text{tr}}$  so that it involves only second derivatives. After transforming to relative Cartesian coordinates we have

$$q_N^{\text{tr}} = \frac{\hbar^2}{24(k_{\text{B}}T)^2} \exp\left(-\frac{V_N}{k_{\text{B}}T}\right) \sum_{i=1}^{N-1} \sum_{j=i+1}^N \frac{1}{\mu_{ij}} \left( \frac{\partial^2 V_{ij}}{\partial x_{ij}^2} + \frac{\partial^2 V_{ij}}{\partial y_{ij}^2} + \frac{\partial^2 V_{ij}}{\partial z_{ij}^2} \right), \quad (18)$$

where  $\mu_{ij}$  is the reduced mass of molecules  $i$  and  $j$ . For Equation (16) a similar derivation yields

$$q_N^{\text{rot}} = \frac{\hbar^2}{24(k_{\text{B}}T)^2} \exp\left(-\frac{V_N}{k_{\text{B}}T}\right) \times \sum_{i=1}^{N-1} \sum_{j=i+1}^N \left[ \frac{1}{I_i} \left( \frac{\partial^2 V_{ij}}{\partial \psi_{i,a}^2} + \frac{\partial^2 V_{ij}}{\partial \psi_{i,b}^2} \right) + \frac{1}{I_j} \left( \frac{\partial^2 V_{ij}}{\partial \psi_{j,a}^2} + \frac{\partial^2 V_{ij}}{\partial \psi_{j,b}^2} \right) \right], \quad (19)$$

where  $\psi_{i,a}$  and  $\psi_{i,b}$  are the angles of rotation around the two principal axes of inertia of molecule  $i$ .

The second and third pressure virial coefficients are related to the configuration integrals by

$$B_2 = -\frac{1}{2V} (Z_2 - Z_1^2) \quad (20)$$

and

$$B_3 = -\frac{1}{3V} (Z_3 - 3Z_2Z_1 + 2Z_1^3) + \frac{1}{V^2} (Z_2 - Z_1^2)^2, \quad (21)$$

where  $Z_1 = V$ . For the second virial coefficient including the first-order quantum correction this leads to

$$B_2^{\text{cl+qc}}(T) = -\frac{1}{2V} \int \cdots \int \langle f_{12} - q_{12} \rangle d\mathbf{R}_1 d\mathbf{R}_2. \quad (22)$$

To obtain the expression for the pairwise-additive third virial coefficient, the  $f_{ij}$  functions in Equation (12) have to be replaced by  $f_{ij} - q_{ij}$ . After expanding, all terms containing more than one  $q_{ij}$  function have to be dropped, since they belong to higher-order quantum corrections. We thus obtain

$$B_{3,\text{add}}^{\text{cl+qc}}(T) = -\frac{1}{3V} \int \cdots \int \langle f_{12}f_{13}f_{23} - q_{12}f_{13}f_{23} - f_{12}q_{13}f_{23} - f_{12}f_{13}q_{23} \rangle \\ \times d\mathbf{R}_1 d\mathbf{R}_2 d\mathbf{R}_3. \quad (23)$$

The quantum correction derived for  $B_{3,\text{add}}^{\text{cl}}$  can also be applied for  $B_{3,\text{nadd}}^{\text{cl}}$ , assuming that the nonadditive contribution to the quantum correction is negligible:

$$B_{3,\text{nadd}}^{\text{cl+qc}}(T) = -\frac{1}{3V} \int \cdots \int \langle f_{123} - f_{12} - f_{13} - f_{23} - f_{12}f_{13}(1 + q_{23}) \\ - f_{12}f_{23}(1 + q_{13}) - f_{13}f_{23}(1 + q_{12}) \rangle d\mathbf{R}_1 d\mathbf{R}_2 d\mathbf{R}_3. \quad (24)$$

### 3.2. Numerical evaluation

We computed the second and third pressure virial coefficients using the Mayer-sampling Monte Carlo (MSMC) approach by Singh and Kofke [51]. In this procedure, a biased  $n$ -particle Monte Carlo simulation is performed for each virial coefficient  $B_n$ . Importance sampling is achieved by using a sampling distribution  $\pi$  that is equal to the absolute value of the integrand  $\tilde{B}_n$  of the considered virial coefficient. Accordingly, trial moves in the MC simulations are accepted with the probability  $\min(1, \pi_{\text{new}}/\pi_{\text{old}})$ . The value of the virial coefficient is then obtained as

$$B_n(T) = B_n^{\text{hs}} \frac{\langle \tilde{B}_n(T)/\pi \rangle_\pi}{\langle \tilde{B}_n^{\text{hs}}/\pi \rangle_\pi}. \quad (25)$$

Here, the superscript *hs* indicates that the hard-sphere fluid was chosen as reference system. The angle brackets represent the simulation averages of the weighted integrands of the realistic potential model,  $\tilde{B}_n(T)/\pi$ , and of the hard-sphere potential,  $\tilde{B}_n^{\text{hs}}/\pi$ , both computed for the same configurations of the particles according to the sampling distribution  $\pi$ . The hard-sphere virial coefficients  $B_2^{\text{hs}}$  and  $B_3^{\text{hs}}$  are known analytically [46].

Virial coefficients for multiple temperatures can be obtained from a single simulation [14, 51], leading to a considerable reduction of the computational costs. In this case, the sampling distribution  $\pi$  is the integrand of the considered virial coefficient

at a sampling temperature  $T_s$ . The only disadvantage of this approach is that for temperatures far away from  $T_s$  the sampling is not optimal. The best results are usually achieved if  $T_s$  is the lowest of the considered temperatures.

The second virial coefficient of  $N_2$  was computed for 96 temperatures between 50 K and 3000 K by performing multi-temperature simulations with  $T_s = 50$  K and  $5 \times 10^{10}$  trial moves. The results from eight independent simulation runs were averaged. For the third virial coefficient 90 temperatures between 80 K and 3000 K were considered with  $T_s = 80$  K. The number of simulation runs and the number of trial moves per simulation run were the same as for the second virial coefficient. For each MC trial move, one molecule was displaced and rotated. The step sizes in the MC moves were adjusted in short equilibration periods to achieve acceptance rates of 50%. A hard-sphere diameter of 4.5 Å was chosen for the reference system. To avoid unphysical values of the realistic pair potential at very short intermolecular distances, a hard-sphere core with a diameter of 2.0 Å was applied. The nonadditive induction contribution,  $\Delta V_{123}^{\text{ind}}$ , was set to zero if one of the centre-of-mass distances between two molecules was larger than 30 Å. For the calculation of the quantum corrections, the second derivatives of the pair potential [see Equations (18) and (19)] were evaluated analytically.

The computed second and third virial coefficients are converged within  $0.02 \text{ cm}^3 \text{ mol}^{-1}$  and  $1 \text{ cm}^6 \text{ mol}^{-2}$ , respectively, for all temperatures. The values obtained with  $V_{12}^{\text{B}}$  for  $B_2^{\text{cl}}$ ,  $B_2^{\text{cl+qc}}$ ,  $B_{3,\text{add}}^{\text{cl}}$ ,  $B_{3,\text{nadd}}^{\text{cl}}$  and  $B_{3,\text{nadd}}^{\text{cl+qc}}$  are given in the supplementary material.

### 3.3. Comparison with experimental data

It is to be taken into account that values for the third pressure virial coefficient  $B_3$  obtained from the analysis of sufficiently accurate measurements are not independent of those for the second pressure virial coefficient  $B_2$ . Therefore, it is preferable to include second and third pressure virial coefficients which were simultaneously derived from the same experiment in the comparison with theoretically calculated values. One recent examination by Dymond *et al.* [52, 53] facilitated the selection of six papers [54–59] that meet this requirement. Moreover, Dymond *et al.* estimated the uncertainties of the reported values of  $B_2$  and  $B_3$  for those papers in which the uncertainties were not specified.

Holborn and Otto [54] as well as Michels *et al.* [55] derived second and at least third pressure virial coefficients from isothermal measurements of volume, density and pressure. On the contrary, Canfield *et al.* [56], Crain and Sonntag [57], Roe [58], as well as Zhang *et al.* [59] used apparatuses of the Burnett type to determine isothermal compression factors and finally second and third pressure virial coefficients. Corresponding to the temperature ranges, the uncertainties of  $B_2$  in  $\text{cm}^3 \text{ mol}^{-1}$  are:  $\pm 1.0$  between 143 and 673 K [54] and between 273 and 423 K

[55],  $\pm(2.0$  to  $1.0)$  from 133 to 273 K [56],  $\pm(0.3$  to  $0.1)$  from 143 to 273 K [57],  $\pm(0.3$  to  $0.2)$  from 156 to 291 K [58] and  $\pm 0.2$  between 269 and 353 K [59]. The uncertainties of  $B_3$  are given in  $\text{cm}^6 \text{mol}^{-2}$  as:  $\pm 30$  [54],  $\pm 60$  [55],  $\pm(50$  to  $40)$  [56],  $\pm(60$  to  $25)$  [57],  $\pm 200$  [58] and  $\pm 100$  [59].

In addition, Nowak *et al.* [60], a paper not considered by Dymond *et al.* [52, 53], reported on very accurate experiments with a high-precision two-sinker densimeter. They conservatively estimated their uncertainties for  $B_2$  to be  $\pm(0.8$  to  $0.3) \text{cm}^3 \text{mol}^{-1}$  between 98 and 123 K and  $\pm 0.25 \text{cm}^3 \text{mol}^{-1}$  from 125 to 340 K. The derived values of  $B_3$  are characterized by uncertainties of  $\pm(800$  to  $150) \text{cm}^6 \text{mol}^{-2}$  between 98 and 130 K and  $\pm 100 \text{cm}^6 \text{mol}^{-2}$  from 133 to 340 K.

Furthermore, values for the second pressure virial coefficient in the temperature range of 75–700 K, inferred by Ewing and Trusler [61] from their data of the second acoustic virial coefficient and recommended by Dymond *et al.* [52], were also considered. Ewing and Trusler measured the speed of sound in nitrogen between 80 and 373 K and determined values of the second acoustic virial coefficient  $\beta_{2a}$  with a very low uncertainty of  $\pm 0.11 \text{cm}^3 \text{mol}^{-1}$ . Subsequently, they derived an empirical anisotropic site-site model of the intermolecular PES of nitrogen, which they used to calculate values for the second pressure virial coefficient in the above mentioned temperature range. The uncertainties are believed to be about  $\pm 0.5 \text{cm}^3 \text{mol}^{-1}$  and  $\pm 0.1 \text{cm}^3 \text{mol}^{-1}$  near the lowest and highest temperatures, respectively. The second acoustic virial coefficient should be more suitable for the validation of the PES than the second pressure virial coefficient due to the lower uncertainty of the former at low temperatures. We obtained second acoustic virial coefficients for the potential function  $V_{12}^B$  using the relation

$$\beta_{2a}(T) = 2 \left[ B_2(T) + [\gamma^\circ(T) - 1]TB_2'(T) + \frac{[\gamma^\circ(T) - 1]^2}{2\gamma^\circ(T)}T^2B_2''(T) \right]. \quad (26)$$

Here,  $\gamma^\circ(T) = c_p^\circ(T)/c_v^\circ(T)$  is the ratio of the isobaric and isochoric heat capacities in the ideal gas limit;  $B_2'(T)$  and  $B_2''(T)$  are the first and second temperature derivatives of  $B_2(T)$ . We used the  $\gamma^\circ$  values of Ewing and Trusler and determined  $B_2(T)$ ,  $B_2'(T)$  and  $B_2''(T)$  from an analytical function fitted to  $B_2^{\text{cl+qc}}(T)$ .

In Figure 3, the selected experimental data for the second pressure virial coefficient ( $B_2^{\text{exp}}$ ) are compared with values calculated using the  $V_{12}^B$  potential function ( $B_2^{\text{cl+qc}}$ ), which were interpolated for the experimental temperatures. The figure, in which the absolute deviations are displayed, demonstrates that practically all data agree with the theoretical values within the estimated uncertainties given above. Apart from three data points, the older data of [54–56] are consistent within  $\pm 0.5 \text{cm}^3 \text{mol}^{-1}$  with the theoretical values, which is much less than the assumed uncertainties. The data of Crain and Sonntag [57] and of Roe [58] coincide with the

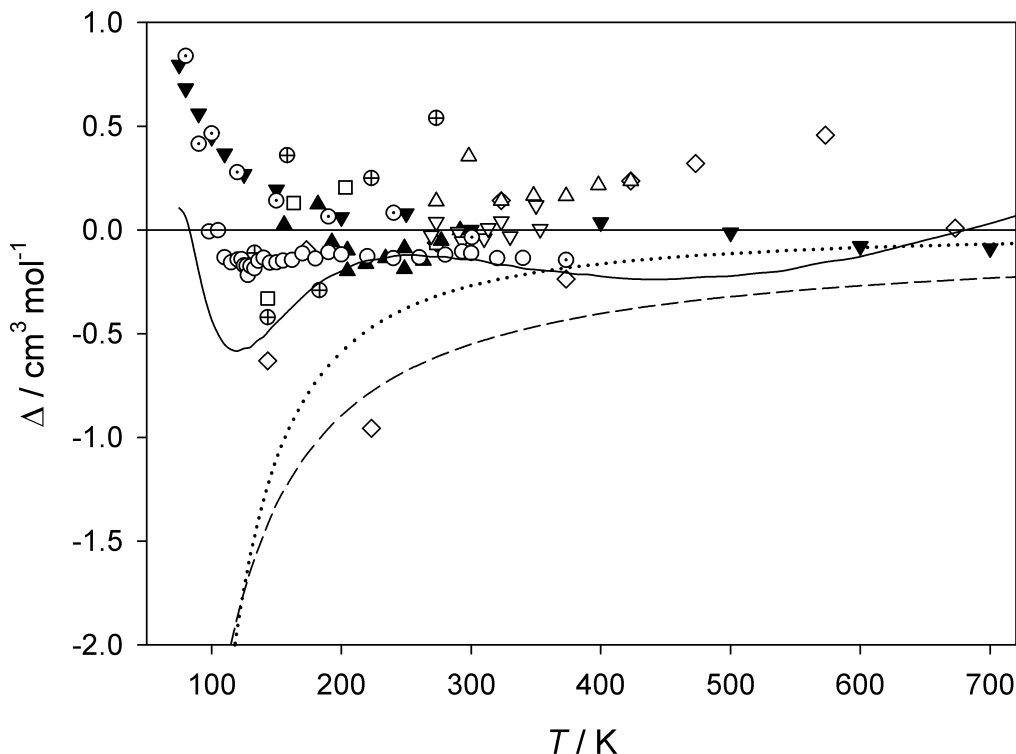


Figure 3. Deviations,  $\Delta = B_2^{\text{exp}} - B_2^{\text{cl+qc}}$ , of experimental second pressure virial coefficients for  $\text{N}_2$  from values calculated with the potential function  $V_{12}^{\text{B}}$  as a function of temperature. Experimental data:  $\diamond$ , Holborn and Otto [54];  $\triangle$ , Michels *et al.* [55];  $\oplus$ , Canfield *et al.* [56];  $\square$ , Crain and Sonntag [57];  $\blacktriangle$ , Roe [58];  $\nabla$ , Zhang *et al.* [59];  $\circ$ , Nowak *et al.* [60]. Experimentally based values:  $\blacktriangledown$ , Ewing and Trusler [61]. Experimentally based correlation: —, Dymond *et al.* [52]. Other calculated values:  $\cdots$ , classical result;  $---$ , potential function  $V_{12}^{\text{A}}$ . Deviations,  $\Delta = \beta_{2a}^{\text{exp}} - \beta_{2a}^{\text{cl+qc}}$ , of experimental second acoustic virial coefficients for  $\text{N}_2$  from values calculated with the potential function  $V_{12}^{\text{B}}$ :  $\odot$ , Ewing and Trusler [61].

theoretical values within their low uncertainties. The agreement with the data of Zhang *et al.* [59] is almost perfect. The data of Nowak *et al.* [60] differ on average by  $-0.15 \text{ cm}^3 \text{ mol}^{-1}$  from the theoretical values apart from two data points at the lowest temperatures. The  $B_2$  values of Ewing and Trusler [61] agree perfectly at high temperatures with the theoretically calculated values and deviate only at temperatures below 90 K by more than  $+0.5 \text{ cm}^3 \text{ mol}^{-1}$ . The deviations for the second acoustic virial coefficients of Ewing and Trusler, which are also shown in the figure, are similar to the deviations for their second pressure virial coefficients. The figure makes also evident that the  $B_2$  correlation recommended by Dymond *et al.* [52] agrees within its uncertainties of  $\pm 1.0 \text{ cm}^3 \text{ mol}^{-1}$  at 75 K,  $\pm 0.2 \text{ cm}^3 \text{ mol}^{-1}$  at room temperature and  $\pm 0.8 \text{ cm}^3 \text{ mol}^{-1}$  at 745 K with the theoretically calculated values.

In Figure 3, the values for the second pressure virial coefficient obtained from the  $V_{12}^{\text{B}}$  potential are additionally compared with those from the  $V_{12}^{\text{A}}$  potential (which was not adjusted to the second pressure virial coefficients). The values resulting from  $V_{12}^{\text{A}}$  are consistently too negative for all temperatures.

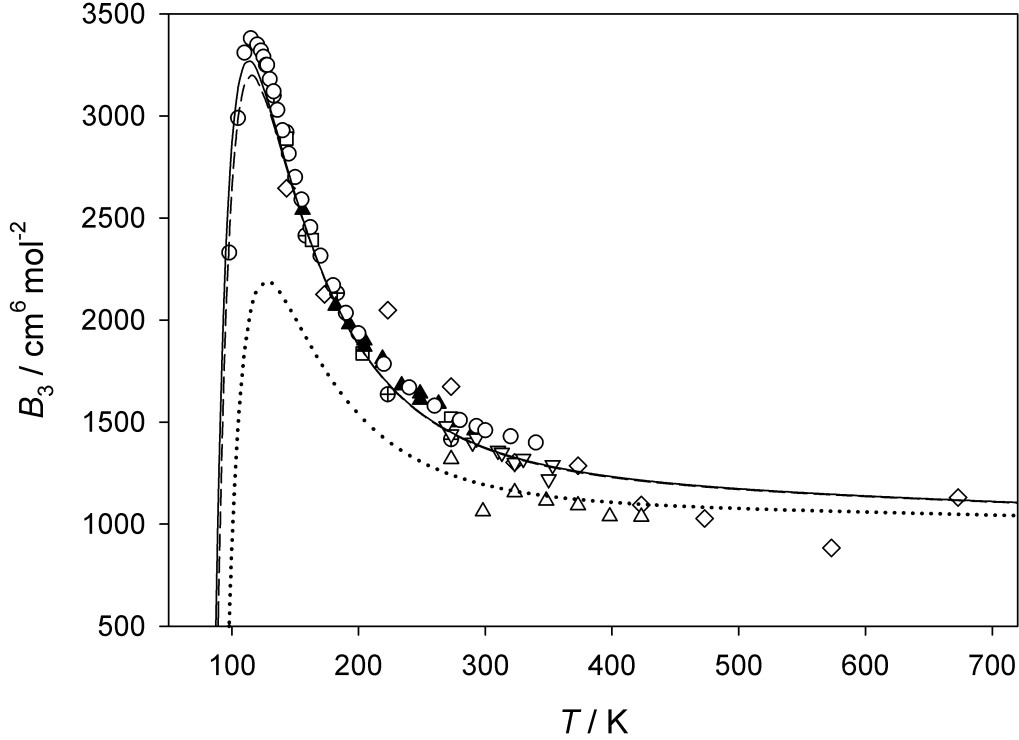


Figure 4. Experimental third pressure virial coefficients for  $N_2$  and values calculated with the potential function  $V_{12}^B$  as a function of temperature. Experimental data:  $\diamond$ , Holborn and Otto [54];  $\triangle$ , Michels *et al.* [55];  $\oplus$ , Canfield *et al.* [56];  $\square$ , Crain and Sonntag [57];  $\blacktriangle$ , Roe [58];  $\nabla$ , Zhang *et al.* [59];  $\circ$ , Nowak *et al.* [60]. Calculated values:  $\cdots$ ,  $B_{3,\text{add}}^{\text{cl}}$ ;  $---$ ,  $B_{3,\text{nadd}}^{\text{cl}}$ ;  $---$ ,  $B_{3,\text{nadd}}^{\text{cl+qc}}$ .

Figure 4 shows the comparison for the third pressure virial coefficient between experimental data and values calculated using the  $V_{12}^B$  potential function. The results obtained with  $V_{12}^A$  are not shown, because the differences to the results obtained with  $V_{12}^B$  are too small to be visible. The figure elucidates that good agreement is only achieved if nonadditive contributions are considered in the calculations, whereas the first-order quantum correction contributes significantly only for the lowest temperatures. The data of Nowak *et al.* [60] agree within the error bars for all temperatures with the theoretical values. Even the maximum of the third pressure virial coefficient at the lowest temperatures is correctly described with differences distinctly smaller than the conservatively estimated uncertainties. As in the case of the second pressure virial coefficient, the  $B_3$  data of Roe [58] are consistent with the theoretical values, those of Zhang *et al.* [59] agree perfectly. The agreement for both data sets is much better than their rather large uncertainty estimates. On the contrary, the theoretical values do not reproduce the experimental data of Canfield *et al.* [56] and of Crain and Sonntag [57] within their low uncertainties, although the agreement is quite reasonable. Only the older data of Holborn and Otto [54] and of Michels *et al.* [55] show larger differences to the theoretical values. This concerns particularly the high-temperature range. Due to the good agreement of the theoretical values

with the more recent experimental data at lower temperatures, we believe that the theoretical results could provide decision guidance at high temperatures.

## 4. Shear viscosity and thermal conductivity

### 4.1. Theory

The shear viscosity  $\eta$  and the thermal conductivity  $\lambda$  of a molecular gas in the limit of zero density can be expressed as [10]

$$\eta(T) = \frac{k_B T}{\langle v \rangle_0} \frac{f_\eta^{(n)}}{\mathfrak{S}(2000)} \quad (27)$$

and

$$\lambda(T) = \frac{5k_B^2 T}{2m\langle v \rangle_0} \frac{\mathfrak{S}(1001) - 2r\mathfrak{S}\left(\begin{smallmatrix} 1001 \\ 1010 \end{smallmatrix}\right) + r^2\mathfrak{S}(1010)}{\mathfrak{S}(1010)\mathfrak{S}(1001) - \mathfrak{S}\left(\begin{smallmatrix} 1001 \\ 1010 \end{smallmatrix}\right)^2} f_\lambda^{(n)}, \quad (28)$$

where  $\langle v \rangle_0 = 4(k_B T / \pi m)^{1/2}$  is the average relative thermal speed. The quantities  $\mathfrak{S}(2000)$ ,  $\mathfrak{S}(1010)$ ,  $\mathfrak{S}(1001)$  and  $\mathfrak{S}\left(\begin{smallmatrix} 1001 \\ 1010 \end{smallmatrix}\right)$  are temperature-dependent generalized cross sections, and the notation and conventions employed are fully described elsewhere [10, 62]. The parameter  $r$  is given by

$$r = \left( \frac{2 c_{\text{int}}^\circ}{5 k_B} \right)^{1/2}, \quad c_{\text{int}}^\circ = c_{\text{rot}}^\circ + c_{\text{vib}}^\circ. \quad (29)$$

Here,  $c_{\text{int}}^\circ$  is the contribution of both the rotational,  $c_{\text{rot}}^\circ$ , and the vibrational,  $c_{\text{vib}}^\circ$ , degrees of freedom to the isochoric heat capacity  $c_V^\circ$  in the ideal gas limit. The quantities  $f_\eta^{(n)}$  and  $f_\lambda^{(n)}$  are  $n$ th-order correction factors that account for the effects of higher basis function terms in the perturbation series expansion of the solution of the Boltzmann equation [10]. They can be expressed in terms of generalized cross sections [10, 62].

### 4.2. Numerical evaluation

The generalized cross sections for the pair potentials  $V_{12}^A$  and  $V_{12}^B$  were computed by means of classical trajectories using a modified version of the TRAJECT software code [63]. The nitrogen molecules were approximated as rigid rotors in the trajectory calculations. For a given total energy, translational plus rotational, classical trajectories describing the collision of two molecules were obtained by integrating Hamilton's equations from pre- to post-collisional values. The total-energy-dependent generalized cross sections can be represented as nine-dimensional integrals over the

initial states. They were calculated for 33 values of the total energy, ranging from 15 K to 60,000 K, by means of a simple Monte Carlo procedure, in which the initial states were generated utilizing pseudo-random numbers. At each energy up to  $2 \times 10^6$  trajectories were computed. The number of trajectories had to be reduced significantly for low energies, because the computational demand to achieve a sufficient accuracy for a given trajectory is increasing as the energy decreases. The final integration over the total energy was performed using Chebyshev quadrature. Some generalized cross sections are strongly influenced by excited vibrational states, which are not accounted for in the classical trajectory calculations with rigid rotors. These cross sections were corrected employing the methodology described in [64].

Values of  $c_V^\circ$  for nitrogen were obtained from the equation of state by Span *et al.* [65]. The higher-order correction factors  $f_\eta^{(n)}$  and  $f_\lambda^{(n)}$  were calculated up to  $n = 3$  and  $n = 2$ , respectively. The corrections amount to at most +0.8% for viscosity and +1.8% for thermal conductivity. The difference between  $f_\eta^{(3)}$  and  $f_\eta^{(2)}$  is always smaller than 0.04%.

Taking into account the Monte Carlo errors of the generalized cross sections and the possible effects of higher-order contributions beyond  $f_\eta^{(3)}$  and  $f_\lambda^{(2)}$ , we estimate that the computed values for shear viscosity and thermal conductivity are converged within 0.1% and 0.2%, respectively. The values obtained with  $V_{12}^B$  for temperatures between 70 and 3000 K can be found in the supplementary material.

#### 4.3. Comparison with experimental data

Since the theoretical values correspond to the zero-density limit, the literature data were recalculated to this limit based on the details given in the papers. Either isothermal data as a function of density were extrapolated to the limit of zero density, mostly by the authors themselves, or individual data at low density were corrected to it using the Rainwater–Friend theory [66] for the initial density dependence of the viscosity and of the thermal conductivity. If necessary, the experimental temperatures were corrected to the temperature scale ITS-90.

In Figure 5, selected viscosity data [67–76] are compared with the theoretical values. At intermediate temperatures, Kestin *et al.* [69], Timrot *et al.* [70] and very recently Vogel [76] used oscillating-disk viscometers consisting mainly or completely of quartz glass to make benefit of its outstanding properties. They performed relative measurements, whereas Evers *et al.* [74] carried out absolute measurements with a rotating-cylinder viscometer. The uncertainties of the data were estimated by the respective authors to be  $\pm(0.1$  to  $0.3)\%$  [69],  $\pm 0.7\%$  [70],  $\pm 0.15\%$  [74] and  $\pm(0.1$  to  $0.2)\%$  [76] in the measured temperature ranges. May *et al.* [75] determined the ratio between the viscosities of nitrogen and helium in the limit of zero density at 298.15 K with an uncertainty of  $\pm 0.018\%$  using a capillary viscometer. The most recent value for the zero-density viscosity of helium at 298.15 K has an extremely

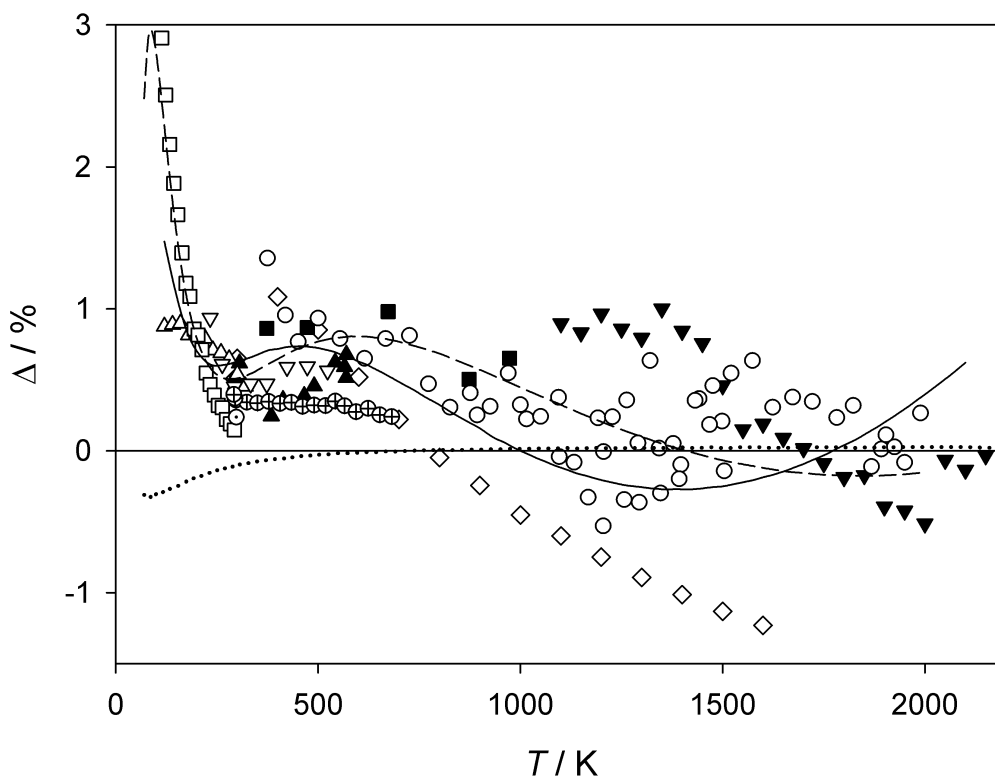


Figure 5. Deviations,  $\Delta = (\eta_{\text{exp}} - \eta_{\text{cal}})/\eta_{\text{cal}}$ , of experimental zero-density viscosities for  $\text{N}_2$  from values calculated with the potential function  $V_{12}^{\text{B}}$  as a function of temperature. Experimental data:  $\blacktriangledown$ , Guevara *et al.* [67];  $\diamond$ , Dawe and Smith [68];  $\blacksquare$ , Kestin *et al.* [69];  $\blacktriangle$ , Timrot *et al.* [70];  $\triangle$ , Gough *et al.* [71];  $\circ$ , Lavushchev and Lyusternik [72];  $\square$ , Lukin *et al.* [73];  $\nabla$ , Evers *et al.* [74];  $\odot$ , May *et al.* [75];  $\oplus$ , Vogel [76]. Experimentally based correlations: —, Vogel *et al.* [77]; ---, Lemmon and Jacobsen [78]. Other calculated values:  $\cdots\cdots$ , potential function  $V_{12}^{\text{A}}$ .

low uncertainty of only  $\pm 0.001\%$  [6], resulting in an uncertainty of  $\pm 0.019\%$  for the zero-density viscosity of nitrogen at 298.15 K. The figure reveals that at room temperature the data of three of the papers are about 0.45% higher than the theoretical values, whereas the data of Vogel and of May *et al.* are higher by only 0.35% and 0.24%, respectively. This is due to the use of theoretically calculated reference values for the viscosity of helium at room temperature for the relative measurements performed by these authors. The figure illustrates that the data of Evers *et al.*, apart from one datum at the lowest temperature, are approximately (0.5 to 0.6)% higher than the calculated values, whereas the data of Timrot *et al.* show the same trend with somewhat smaller differences between about 380 and 470 K. The recent data by Vogel are characterized by practically the same temperature function as the theoretically computed values, but shifted by about  $+(0.35 \text{ to } 0.25)\%$ . Furthermore, the figure elucidates that the deviations of the data by Kestin *et al.* increase up to 1% between 370 and 570 K.

At very high temperatures, Guevara *et al.* [67] and Dawe and Smith [68] carried

out measurements with capillary viscometers and claimed uncertainties of  $\pm 0.4\%$  and  $\pm 1\%$ . Lavushchev and Lyusternik [72] used the flow through a porous medium for their high-temperature experiments and estimated the uncertainty to be  $\pm 1\%$ . All these measurements were performed relative to reference values for the viscosity of nitrogen near room temperature. Figure 5 reveals that the data of Dawe and Smith decrease systematically with increasing temperature beyond the claimed uncertainty of  $\pm 1\%$ . Considering a possible shift of the theoretically calculated viscosity values of the present paper by about  $0.3\%$  to higher values, a close agreement with the data of Guevara *et al.* and of Lavushchev and Lyusternik (apart from one datum at the lowest temperature) is found up to temperatures of 2100 K.

At low temperatures, capillary viscometers were used by Gough *et al.* [71] for relative measurements and by Lukin *et al.* [73] for absolute ones. Gough *et al.* calibrated their viscometer with a reference value for the viscosity of nitrogen at room temperature and estimated the uncertainty to be  $\pm 1\%$  at 120 K. Lukin *et al.* claimed the uncertainty of their results to be  $\pm(0.1 \text{ to } 0.3)\%$ . Figure 5 makes evident that these low-temperature data do not agree within their mutual uncertainties. In addition, the data of Lukin *et al.* deviate up to about  $+3\%$  below 100 K from the theoretical values, whereas the data of Gough *et al.* are consistent with them down to 120 K.

The theoretical values were further compared with experimentally based reference values of Vogel *et al.* [77] and of Lemmon and Jacobsen [78]. Vogel *et al.* conservatively claimed the uncertainty of their correlated values to be  $\pm 0.3\%$  at room temperature, rising to  $\pm 0.5\%$  at 1000 K and  $\pm 2\%$  at 120 and 2100 K. The uncertainty of the correlation of Lemmon and Jacobsen was estimated by the authors to be  $\pm 0.5\%$  in the dilute-gas region. Figure 5 reveals that at high temperatures both correlations represent the experimental data very well and are in close agreement with the theoretically calculated values, even if a shift of  $+0.3\%$  is considered. However, at low temperatures around 100 K, both correlations differ strongly. The reason is that Vogel *et al.* did not take into account the data of Lukin *et al.* [73]. It is obvious that the correlations cannot assist in any decision which data are more reliable. But the theoretical values give more insight into solving this problem. We are convinced that the temperature dependence of the theoretical values could help to resolve the extrapolation problems to high and particularly to low temperatures at which the measurements are more difficult.

In Figure 6, selected thermal conductivity data [79–93] are compared with the theoretical values. The transient hot-wire (THW) technique was applied in seven of the fifteen papers [83, 85–87, 91–93], the steady-state hot-wire (SHW) technique in three [79, 82, 84]. The concentric-cylinder (CC) method was employed by three groups of researchers [80, 81, 88], whereas the shock-tube (ST) technique [89] and a guarded parallel-plate (PP) apparatus [90] were used by one in each case.

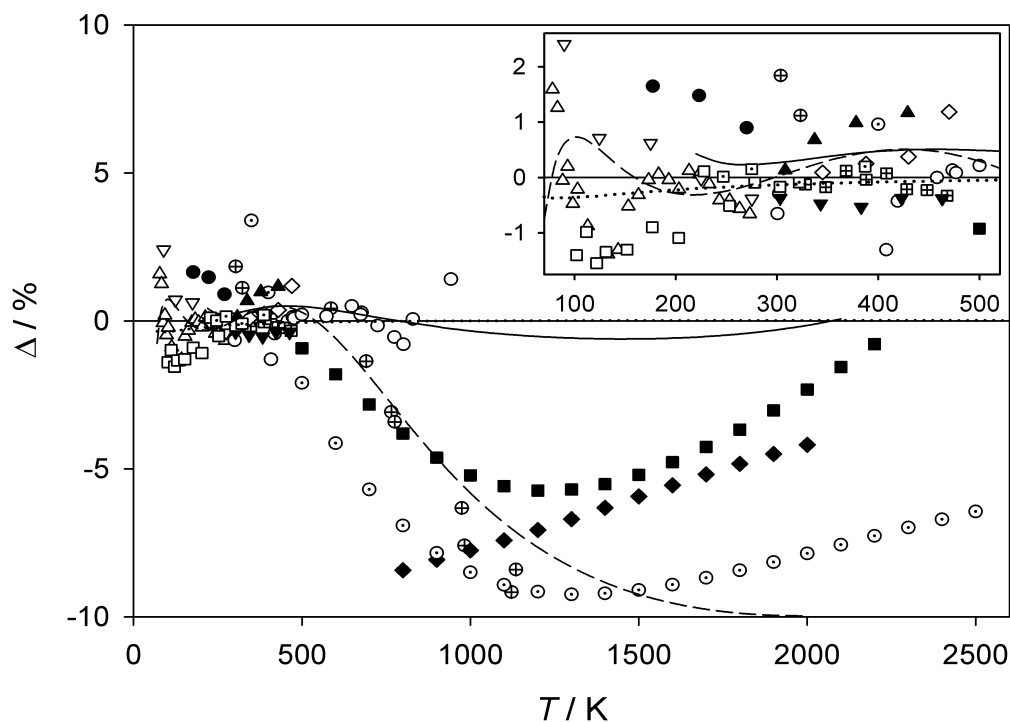


Figure 6. Deviations,  $\Delta = (\lambda_{\text{exp}} - \lambda_{\text{cal}})/\lambda_{\text{cal}}$ , of experimental zero-density thermal conductivities for  $\text{N}_2$  from values calculated with the potential function  $V_{12}^{\text{B}}$  as a function of temperature. Experimental data:  $\oplus$ , Vargaftik and Zimina [79];  $\Delta$ , Golubev and Kalsina [80];  $\circ$ , Le Neindre [81];  $\blacklozenge$ , Faubert and Springer [82];  $\boxplus$ , Haarman [83];  $\odot$ , Saxena and Chen [84];  $\blacktriangle$ , Haran *et al.* [85];  $\diamond$ , Johns *et al.* [86, 87];  $\nabla$ , Zarev *et al.* [88];  $\blacksquare$ , Hoshino *et al.* [89];  $\blacktriangledown$ , Hemminger [90];  $\bullet$ , Millat *et al.* [91];  $\square$ , Perkins *et al.* [92];  $\square$ , Li *et al.* [93]. Experimentally based correlations: —, Millat and Wakeham [94]; - - -, Lemmon and Jacobsen [78]. Other calculated values:  $\cdots\cdots$ , potential function  $V_{12}^{\text{A}}$ .

The THW measurements of Haran *et al.* [85] and of Li *et al.* [93] near to room temperature yielded data which differ from the calculated values by less than +0.2%. These differences correspond approximately to the uncertainties of  $\pm 0.3\%$  estimated by most of the THW experimenters. An inspection of the experimental data obtained away from ambient temperature is more revealing. The data of Haran *et al.* and of Johns *et al.* [86, 87] are characterized by increasing differences up to +1.2% at 429 K and at 470 K, respectively. The data of Millat *et al.* [91] show increasingly positive deviations up to +1.65% at temperatures down to 178 K. On the contrary, the experimental data of Haarman [83] and Li *et al.* [93], derived from THW measurements at rather low pressures, are characterized by deviations of +0.12% to  $-0.33\%$  between 328 and 468 K and of  $-0.1\%$  to +0.2% between 247 and 387 K, respectively. The temperature dependencies of these two data sets correspond closely to that of the calculated values. The same is valid for the results of the PP measurements of Hemminger [90] from room temperature up to 463 K, which exhibit deviations from the theoretical values between  $-0.37\%$  and  $-0.53\%$ .

Figure 6 reveals that the situation becomes somewhat more complicated at low

temperatures. The data of Perkins *et al.* [92], who assessed the uncertainty of their THW measurements to be  $\pm 1\%$  down to 103 K, are 1 to 1.5% lower than the theoretical values at temperatures below 200 K. The uncertainty of the SHW technique is expected to be  $\pm(1 \text{ to } 2)\%$  at most for measurements at low temperatures. In accordance with this, the SHW data of Golubev and Kalsina [80] agree within  $\pm 1.6\%$  with the theoretical values from room temperature down to 78 K. For the comparison the data of Golubev and Kalsina, measured at atmospheric pressure, had to be corrected to the limit of zero density by about  $-2\%$  below 100 K using the Rainwater–Friend theory [66]. Note that the correction is of the same order for the CC measurements of Zarev *et al.* [88], for which the measured isotherms were extrapolated to the zero-density limit yielding practically the same values. The results of Zarev *et al.* show the largest difference from the calculated values with  $+2.4\%$  at the lowest temperature of 90 K.

The comparison at high temperatures is disappointing, apart from the CC data of Le Neindre [81]. He estimated the uncertainty of his measurements to be  $\pm 2.5\%$ , whereas the deviations from the theoretical values amount to only  $\pm 1.4\%$  at most between 300 and 942 K. In contrast, the SHW data of Vargaftik and Zimina [79] and of Saxena and Chen [84] differ by  $-9.2\%$  from the theoretically calculated values at 1120 K and at 1300 K, respectively. The deviations decrease with decreasing temperature and become positive with  $+1.8\%$  at 303 K for [79] and  $+3.4\%$  at 350 K for [84]. The SHW measurements of Faubert and Springer [82] show large negative deviations of  $-8.4\%$  at 800 K decreasing to  $-4.2\%$  at 2000 K. All these differences should be compared with the uncertainties estimated by the authors, which are  $\pm 3\%$  for [79, 82] and  $\pm 1.5\%$  for [84]. Finally, Hoshino *et al.* [89] obtained data with the ST technique between 500 and 2200 K which follow the trend of the discussed SHW data. The largest deviation is  $-5.7\%$  at 1200 K.

In addition, Figure 6 shows a comparison with two thermal-conductivity correlations. The figure makes evident that at high temperatures the correlation of Lemmon and Jacobsen [78] is exclusively based on the experimental data so that differences of  $-10\%$  occur at 2000 K. On the contrary, the temperature functions of the correlation by Millat and Wakeham [94] and of the theoretically calculated values are consistent within  $\pm 0.6\%$  over the whole temperature range from 220 to 2100 K. This is much less than the estimated uncertainty of  $\pm 2.5\%$  at the low- and high-temperature extremes of the correlation. The excellent agreement at high temperatures is certainly based on the fact that Millat and Wakeham used some theoretical guidance from the kinetic theory of gases for their correlation.

## 5. Summary and conclusions

A new four-dimensional intermolecular potential energy hypersurface for two rigid nitrogen molecules was determined from highly accurate quantum-chemical *ab initio* computations. Interaction energies for 408 configurations of two nitrogen molecules were calculated at the CCSD(T) level of theory using basis sets up to aug-cc-pV5Z with bond functions. The resulting interaction energies were extrapolated to the complete basis set limit. Furthermore, corrections for core-core and core-valence correlations, relativistic effects and higher coupled-cluster levels up to CCSDT(Q) were computed. A site-site potential function with five sites per molecule was fitted to the calculated interaction energies.

The new potential function was used to compute the second and third pressure virial coefficients as well as shear viscosity and thermal conductivity in the dilute-gas limit. Using the most accurate experimental data for the second virial coefficient as guidance, the potential was further improved by scaling the CCSDT(Q) correction for all interaction energies by a factor of 0.5 and refitting the potential parameters. The influence of this adjustment on the other three properties is very small.

The second and third pressure virial coefficients for temperatures up to 3000 K were calculated classically with the first-order translational and rotational quantum corrections using the Mayer-sampling Monte Carlo approach. In the case of the third virial coefficient nonadditive dispersion and induction contributions were also taken into account. The quantum correction to the third virial coefficient for rigid linear molecules and pairwise-additive potentials was derived in this paper. The extension to nonlinear molecules and higher virial coefficients is straightforward. For both the second and the third pressure virial coefficient the agreement with the most accurate experimental data turned out to be excellent.

Shear viscosity and thermal conductivity in the dilute-gas limit were computed for temperatures between 70 and 3000 K using the kinetic theory of molecular gases and the classical trajectory method. For shear viscosity the comparison with the most accurate experimental data indicated that the calculated values are too low by about 0.3% between 300–700 K. Apart from this shift, which is probably caused by the deficiencies of the rigid-rotor approximation, the agreement is excellent. Hence, we recommend to scale the computed viscosity values for all temperatures by a factor of 1.003 to obtain reference values. The computed thermal conductivity values are in very good agreement with the experimental data for temperatures below 500 K. However, at higher temperatures most of the experimental data show large negative deviations (up to  $-9\%$ ) from the theoretically calculated values. Considering the very good agreement between theory and experiment for the thermal conductivity below 500 K as well as for the virial coefficients and shear viscosity, it is highly unlikely that the theoretically calculated values for the thermal conduc-

tivity are characterized by such large uncertainties. Therefore, the computed values are recommended as reference values for the complete temperature range.

### Acknowledgment

I am grateful to Professor Eckhard Vogel for assistance with the assessment of the experimental data.

### References

- [1] R. Hellmann, E. Bich and E. Vogel, *Mol. Phys.* **105** (23-24), 3013 (2007).
- [2] R. Hellmann, E. Bich and E. Vogel, *Mol. Phys.* **106** (1), 133 (2008).
- [3] B. Jäger, R. Hellmann, E. Bich and E. Vogel, *Mol. Phys.* **107** (20), 2181 (2009).
- [4] B. Jäger, R. Hellmann, E. Bich and E. Vogel, *Mol. Phys.* **108** (1), 105 (2010).
- [5] K. Patkowski and K. Szalewicz, *J. Chem. Phys.* **133** (9), 094304 (2010).
- [6] W. Cencek, M. Przybytek, J. Komasa, J.B. Mehl, B. Jeziorski and K. Szalewicz, *J. Chem. Phys.* **136** (22), 224303 (2012).
- [7] R. Hellmann, E. Bich and E. Vogel, *J. Chem. Phys.* **128** (21), 214303 (2008).
- [8] R. Bukowski, K. Szalewicz, G.C. Groenenboom and A. van der Avoird, *J. Chem. Phys.* **128** (9), 094314 (2008).
- [9] R. Hellmann, E. Bich, E. Vogel and V. Vesovic, *Phys. Chem. Chem. Phys.* **13** (30), 13749 (2011).
- [10] F.R.W. McCourt, J.J.M. Beenakker, W.E. Köhler and I. Kučšer, *Nonequilibrium Phenomena in Polyatomic Gases*, Vol. I: Dilute Gases (Clarendon Press, Oxford, 1990).
- [11] J. Vrabec, J. Stoll and H. Hasse, *J. Phys. Chem. B* **105** (48), 12126 (2001).
- [12] J.J. Potoff and J.I. Siepmann, *AIChE Journal* **47** (7), 1676 (2001).
- [13] M.T. Oakley and R.J. Wheatley, *J. Chem. Phys.* **130** (3), 034110 (2009).
- [14] B. Jäger, R. Hellmann, E. Bich and E. Vogel, *J. Chem. Phys.* **135** (8), 084308 (2011).
- [15] H.J. Böhm and R. Ahlrichs, *Mol. Phys.* **55** (5), 1159 (1985).
- [16] R. Ahlrichs, P. Scharf and C. Ehrhardt, *J. Chem. Phys.* **82** (2), 890 (1985).
- [17] A. van der Avoird, P.E.S. Wormer and A.P.J. Jansen, *J. Chem. Phys.* **84** (3), 1629 (1986).
- [18] F. Visser, P.E.S. Wormer and P. Stam, *J. Chem. Phys.* **79** (10), 4973 (1983).
- [19] D. Cappelletti, F. Vecchiocattivi, F. Pirani, E.L. Heck and A.S. Dickinson, *Mol. Phys.* **93** (3), 485 (1998).
- [20] C. Amovilli and R. McWeeny, *Chem. Phys.* **140** (3), 343 (1990).
- [21] J.R. Stallcop and H. Partridge, *Chem. Phys. Lett.* **281** (1-3), 212 (1997).
- [22] K. Raghavachari, G.W. Trucks, J.A. Pople and M. Head-Gordon, *Chem. Phys. Lett.* **157** (6), 479 (1989).
- [23] K. Leonhard and U.K. Deiters, *Mol. Phys.* **100** (15), 2571 (2002).
- [24] T.H. Dunning, Jr., *J. Chem. Phys.* **90** (2), 1007 (1989).
- [25] R.A. Kendall, T.H. Dunning, Jr. and R.J. Harrison, *J. Chem. Phys.* **96** (9), 6796 (1992).
- [26] M.H. Karimi-Jafari, A. Maghari and S. Shahbazian, *Chem. Phys.* **314** (1-3), 249 (2005).
- [27] L. Gomez, B. Bussery-Honvault, T. Cauchy, M. Bartolomei, D. Cappelletti and F. Pirani, *Chem. Phys. Lett.* **445** (4-6), 99 (2007).
- [28] P. Strak and S. Krukowski, *J. Chem. Phys.* **126** (19), 194501 (2007).
- [29] Y.J. Bomble, J.F. Stanton, M. Kállay and J. Gauss, *J. Chem. Phys.* **123** (5), 1 (2005).

- [30] C.F. Curtiss, *J. Chem. Phys.* **75** (3), 1341 (1981).
- [31] E.M. Mas and K. Szalewicz, *J. Chem. Phys.* **104** (19), 7606 (1996).
- [32] K.A. Peterson and T.H. Dunning, Jr., *J. Chem. Phys.* **117** (23), 10548 (2002).
- [33] J. Bendtsen, *J. Raman Spectrosc.* **2** (2), 133 (1974).
- [34] S.F. Boys and F. Bernardi, *Mol. Phys.* **19** (4), 553 (1970).
- [35] A. Halkier, T. Helgaker, P. Jørgensen, W. Klopper, H. Koch, J. Olsen and A.K. Wilson, *Chem. Phys. Lett.* **286** (3-4), 243 (1998).
- [36] W. Kutzelnigg, E. Ottschowski and R. Franke, *J. Chem. Phys.* **102** (4), 1740 (1995).
- [37] W. Klopper, *J. Comp. Chem.* **18** (1), 20 (1997).
- [38] CFOUR, Coupled-Cluster techniques for Computational Chemistry, a quantum-chemical program package by J. F. Stanton, J. Gauss, M. E. Harding, P. G. Szalay with contributions from A. A. Auer, R. J. Bartlett, U. Benedikt, C. Berger, D. E. Bernholdt, Y. J. Bomble, O. Christiansen, M. Heckert, O. Heun, C. Huber, T.-C. Jagau, D. Jonsson, J. Jusélius, K. Klein, W. J. Lauderdale, D. A. Matthews, T. Metzroth, D. P. O'Neill, D. R. Price, E. Prochnow, K. Ruud, F. Schiffmann, S. Stopkowitz, A. Tajti, J. Vázquez, F. Wang, J. D. Watts and the integral packages MOLECULE (J. Almlöf and P. R. Taylor), PROPS (P. R. Taylor), ABACUS (T. Helgaker, H. J. Aa. Jensen, P. Jørgensen, and J. Olsen), and ECP routines by A. V. Mitin and C. van Wüllen. For the current version, see <http://www.cfour.de>.
- [39] MRCC, a string-based general coupled cluster program suite written by M. Kállay. See also M. Kállay and P. R. Surján, *J. Chem. Phys.* **115**, 2945 (2001) as well as: <http://www.mrcc.hu>.
- [40] K.T. Tang and J.P. Toennies, *J. Chem. Phys.* **80** (8), 3726 (1984).
- [41] G.D. Zeiss and W.J. Meath, *Mol. Phys.* **33** (4), 1155 (1977).
- [42] H. Li and R.J. Le Roy, *J. Chem. Phys.* **126** (22), 224301 (2007).
- [43] B.M. Axilrod and E. Teller, *J. Chem. Phys.* **11** (6), 299 (1943).
- [44] Y. Muto, *Nippon Sugaku-Buturigakkwaishi* **17** (10-11-12), 629 (1943).
- [45] S.A.C. McDowell and W.J. Meath, *Mol. Phys.* **90** (5), 713 (1997).
- [46] E.A. Mason and T.H. Spurling, *The Virial Equation of State, International Encyclopedia of Physical Chemistry and Chemical Physics, Topic 10: The Fluid State*, Vol. 2 (Pergamon, Oxford, 1969).
- [47] R. Hellmann and E. Bich, *J. Chem. Phys.* **135** (8), 084117 (2011).
- [48] R.T. Pack, *J. Chem. Phys.* **78** (12), 7217 (1983).
- [49] P.E.S. Wormer, *J. Chem. Phys.* **122** (18), 184301 (2005).
- [50] S.K. Singh, N. Prasad and S.K. Sinha, *Physica A* **179** (3), 378 (1991).
- [51] J.K. Singh and D.A. Kofke, *Phys. Rev. Lett.* **92** (22), 220601 (2004).
- [52] J.H. Dymond, R.C. Wilhoit, K.N. Marsh and K.C. Wong, in , edited by M. Frenkel and K. N. Marsh (Springer, Berlin–Heidelberg–New York, 2002), *Group IV: Physical Chemistry*, Vol. 21A: Virial Coefficients of Pure Gases, Chap. 2, pp. 69–72.
- [53] J.H. Dymond, R.C. Wilhoit, K.N. Marsh and K.C. Wong, in , edited by M. Frenkel and K. N. Marsh (Springer, Berlin–Heidelberg–New York, 2002), *Group IV: Physical Chemistry*, Vol. 21A: Virial Coefficients of Pure Gases, Chap. 4, pp. 261–262.
- [54] L. Holborn and J. Otto, *Z. Phys.* **33**, 1 (1925).
- [55] A. Michels, R.J. Lunbeck and G.J. Wolkers, *Physica* **17** (9), 801 (1951).
- [56] F.B. Canfield, T.W. Leland and R. Kobayashi, *Advan. Cryog. Eng.* **8**, 146 (1963).
- [57] R.W. Crain, Jr. and R.E. Sonntag, *Adv. Cryog. Eng.* **11**, 379 (1966).
- [58] D.R. Roe, Ph.D. thesis, University of London London, UK, 1972.
- [59] W. Zhang, J.A. Schouten, H.M. Hinze and M. Jaeschke, *J. Chem. Eng. Data* **37** (1), 114 (1992).
- [60] P. Nowak, R. Kleinrahn and W. Wagner, *J. Chem. Thermodyn.* **29** (10), 1137 (1997).

- [61] M.B. Ewing and J.P.M. Trusler, *Physica A* **184** (3-4), 415 (1992).
- [62] R. Hellmann, E. Bich, E. Vogel, A.S. Dickinson and V. Vesovic, *J. Chem. Phys.* **129** (6), 064302 (2008).
- [63] E.L. Heck and A.S. Dickinson, *Comput. Phys. Commun.* **95** (2-3), 190 (1996).
- [64] S. Bock, E. Bich, E. Vogel, A.S. Dickinson and V. Vesovic, *J. Chem. Phys.* **120** (17), 7987 (2004).
- [65] R. Span, E.W. Lemmon, R.T. Jacobsen, W. Wagner and A. Yokozeki, *J. Phys. Chem. Ref. Data* **29** (6), 1361 (2000).
- [66] E. Bich and E. Vogel, in , edited by J. Millat, J. H. Dymond and C. A. Nieto de Castro (Cambridge University Press, Cambridge, 1996), Chap. 5.2, pp. 72–82.
- [67] F.A. Guevara, B.B. McIntere and W.E. Wageman, *Phys. Fluids* **12** (12), 2493 (1969).
- [68] R.A. Dawe and E.B. Smith, *J. Chem. Phys.* **52** (2), 693 (1970).
- [69] J. Kestin, S.T. Ro and W.A. Wakeham, *J. Chem. Phys.* **56** (12), 5837 (1972).
- [70] D.L. Timrot, M.A. Serednitskaya and S.A. Traktueva, *Teploenergetika* **22** (3), 84 (1975).
- [71] D.W. Gough, G.P. Matthews and E.B. Smith, *J. Chem. Soc., Faraday Trans. 1* **72** (0), 645 (1976).
- [72] A.V. Lavushchev and V.E. Lyusternik, *Teplofiz. Vys. Temp.* **16**, 209 (1978).
- [73] V.I. Lukin, B.A. Ivakin and P.E. Suetin, *Zh. Tekh. Fiz.* **53**, 931 (1983).
- [74] C. Evers, H.W. Losch and W. Wagner, *Int. J. Thermophys.* **23** (6), 1411 (2002).
- [75] E.F. May, R.F. Berg and M.R. Moldover, *Int. J. Thermophys.* **28** (4), 1085 (2007).
- [76] E. Vogel, *Int. J. Thermophys.* **33** (5), 741 (2012).
- [77] E. Vogel, T. Strehlow, J. Millat and W.A. Wakeham, *Z. phys. Chemie (Leipzig)* **270**, 1145 (1989).
- [78] E.W. Lemmon and R.T. Jacobsen, *Int. J. Thermophys.* **25** (1), 21 (2004).
- [79] N.B. Vargaftik and N.K. Zimina, *Teplofiz. Vys. Temp.* **2** (6), 869 (1964).
- [80] I.F. Golubev and M.V. Kalsina, *Gaz. Prom.* **9**, 41 (1964).
- [81] B. Le Neindre, *Int. J. Heat Mass Transfer* **15**, 1 (1972).
- [82] F.M. Faubert and G.S. Springer, *J. Chem. Phys.* **57** (6), 2333 (1972).
- [83] J.W. Haarman, *Am. Inst. Phys. Conf. Proc.* **11**, 193 (1973).
- [84] S.C. Saxena and S.H.P. Chen, *Mol. Phys.* **29** (5), 1507 (1975).
- [85] E.N. Haran, G.C. Maitland, M. Mustafa and W.A. Wakeham, *Ber. Bunsenges. Phys. Chem.* **87** (8), 657 (1983).
- [86] A.I. Johns, S. Rashid, J.T.R. Watson and A.A. Clifford, *J. Chem. Soc., Faraday Trans. 1* **82** (7), 2235 (1986).
- [87] A.I. Johns, S. Rashid, L. Rowan, J.T.R. Watson and A.A. Clifford, *Int. J. Thermophys.* **9** (1), 3 (1988).
- [88] V.V. Zarev, D.N. Nagorov, V.A. Nikonorov and V.N. Popov, in (*Sbornik nauchnyh trudov, Moskva, 1986*), Vol. 114, pp. 5–9.
- [89] T. Hoshino, K. Mito, A. Nagashima and M. Miyata, *Int. J. Thermophys.* **7** (3), 647 (1986).
- [90] W. Hemminger, *Int. J. Thermophys.* **8** (3), 317 (1987).
- [91] J. Millat, M.J. Ross and W.A. Wakeham, *Physica A* **159** (1), 28 (1989).
- [92] R.A. Perkins, H.M. Roder, D.G. Friend and C.A. Nieto de Castro, *Physica A* **173** (3), 332 (1991).
- [93] S.F.Y. Li, M. Papadaki and W.A. Wakeham, Thermal Conductivity of low-density polyatomic gases. in *Proc. 22nd International Thermal Conductivity Conference, (Tempe, Arizona, 1993)*, edited by T. W. Tong (Technomic Publishing Company, Lancaster, PA, 1994), pp. 531–543.
- [94] J. Millat and W.A. Wakeham, *J. Phys. Chem. Ref. Data* **18** (2), 565 (1989).